



Porous structure studies of the mixed-matrix polymeric membranes of polyether sulfone incorporated with functionalized multiwalled carbon nanotubes

Km Nikita^a, S. Kumar^b, V.K. Aswal^b, D.K. Kanchan^c, C.N. Murthy^{a,*}

^aApplied Chemistry Department, Faculty of Technology and Engineering, The M. S. University of Baroda, Vadodara, India, emails: chivukula_mn@yahoo.com (C.N. Murthy), nikitatiwari.m34@gmail.com (K. Nikita)

^bSolid State Physics Division, Bhabha Atomic Research Centre, Mumbai, India, emails: sugamkumar86@gmail.com (S. Kumar), vkaswal@barc.gov.in (V.K. Aswal)

^cDepartment of Physics, The M. S. University of Baroda, Vadodara, India, email: d_k_kanchan@yahoo.com

Received 11 October 2018; Accepted 13 December 2018

ABSTRACT

To overcome the limitation of polymeric and ceramic membranes in terms of performance and durability for water treatment, mixed-matrix membranes are being increasingly studied. In our studies, mixed matrix membranes of functionalized multiwalled carbon nanotubes (MWCNTs) with polyether sulfone as the membrane matrix showed reduced porosity. The pore dimensions, when studied by small angle neutron scattering and capillary flow porometry techniques, showed smaller pores. The cross sectional image of cold fractured membrane obtained from scanning electron microscopy showed that they retained their original asymmetric nature when cast by the phase inversion technique. The thermogravimetric analysis of mixed-matrix membranes showed enhanced thermal properties and better stability to degradation than the pristine membranes with no loss in the stability. These membranes showed better separation characteristics and enhanced selectivity for metal ion separation. Interestingly, the conductivity in dry state of the mixed-matrix membranes showed perfectly semicircular plots which shows conducting nature of the membranes which is attributed to the presence of functionalized nanotubes in the otherwise insulating polymer matrix.

Keywords: Multiwalled carbon nanotubes; Asymmetric; Small angle neutron scattering

1. Introduction

Polyethersulfone (PES) is a versatile polymer extensively used in desalination and also wastewater treatment and has superior properties such as resistance to hydrolysis, dimensional stability and outstanding surface quality [1]. Pristine PES has also been chemically modified to overcome its inherent characteristic of being highly hydrophobic leading to rapid fouling and thus effecting its separation capability [2]. Various studies have shown that hydrophobicity is the cause of membrane fouling which can be mitigated by increasing the hydrophilicity of the

membrane surface [3]. Adsorption of non-polar solutes, hydrophobic particles or bacteria which occupy the pores on the membrane surface is the major cause of fouling thus leading to reduction in the life of the membranes and therefore needs higher energy for the functioning and so the reduced separation efficiency [2]. Subsequent to the Loeb and Sourirajan [4] asymmetric membranes, thin film composite membranes were first devised by Cadotte et al. [5] to overcome the problem of fouling with limited success. Another drawback of these membranes is their sensitivity to chlorine. To overcome this problem, mixed-matrix membranes were developed, though initially for gas separation.

* Corresponding author.

Zimmerman et al. [6] showed that mixed-matrix membrane with carbon molecular sieve in a polysulfone matrix could be used for O₂/N₂ separation. The separation was determined by the size of the zeolites aperture which was in the range of 3.8 Å. Subsequently the idea of mixed-matrix membranes was used for desalination/water treatment. The dispersed phase used were BaCO₃ nanoparticles [7], ZnO nanoparticles [8], silica [9], Ag nanoparticles [10], graphene oxide [11] and multiwalled carbon nanotubes (MWCNTs) [12] apart from polymeric dispersed phase such as polyaniline [13] and poly(sodium 4-styrenesulfonate) [14]. In most of these mentioned dispersed phases, the matrix was either polysulfone/PES or polyvinylidene fluoride prepared by the phase inversion process from a solvent. However, there is no uniformity in the pore sizes reported and in fact there are contradictory results. Some report a reduction in the pore dimensions as compared with the pristine matrix [12,14], some report an increase in the pore dimensions [8,13] and one report mentions no change in the pore dimensions [10]. Yet, the mixed-matrix membrane performance with respect to pure water flux was found to be enhanced in all the cases [8,10,12–14]. Therefore, there is no clarity on the role of the pores in the mixed-matrix membranes even as the above-mentioned references show that polymer-based mixed-matrix membranes which comprise of a polymer continuous phase and a dispersed phase (zeolites, porous silica, carbon molecular sieves, carbon nanotubes, etc.) provides promising solution of low permeation to salt/contaminant and high water flux, higher mechanical strength and also thermal stability. Incorporation of carbon nanotubes (CNTs) is also an attractive approach for designing of new membranes for advanced molecular separation because of their unique transport properties [15] and ability to mimic biological protein channels [16]. MWCNT are attractive for advanced membrane technology since they contain uniform robust pores and provide low energy consumption in the water desalination process [17]. The smooth hydrophobic walls, the inner hollow cavity and inner pore diameter of CNT allow ultra efficient transport of water molecules which provides a great possibility for desalinating water [18]. There are many studies regarding the use of CNTs in polymer matrices for water treatment though the reason of the efficient separation of contaminants in water is not well understood yet. For example, preparation of MWCNT/nanoporous alumina mixed-matrix membranes is reported where nanotubes were grown on the nanoporous alumina template by the chemical vapour deposition method resulting in pore dimensions of as large as 200 nm, and the transport properties of these membranes were explored by the diffusion of rose bengal dye through the membranes [19]. MWCNT immobilized on polyvinylidene difluoride (PVDF) mixed-matrix membranes were used for the removal of volatile organics from air and the presence of CNTs resulted in higher permeation and faster mass-transfer rate as compared with the pristine PVDF [20]. Here too, there is no mention of any pore dimensions and the reasons for higher mass transport, that is, whether the transport is through the CNTs or due to the porous structure of PVDF. Studies also show that nano hybrid membrane of electrically aligned functionalized MWCNT with sulfonated polyether ether ketone show higher proton conductivity due to the creation

of pores facilitating proton conductivity, though the pore dimensions are not reported [21]. Polyamide/functionalized MWCNT membrane prepared by interfacial polymerization could show improved water flux and rejection tendency towards the NaCl due to the pores; however no mention is there about the pore structure [22]. Using PES as a matrix, it was found that the MWCNT/PES membrane had increased porosity as compared with the pristine PES leading to higher water flux though there is no quantification on either the pore size or the porosity [23]. A study regarding protein fouling behaviour of MWCNT/PES mixed-matrix membrane during water filtration showed that the CNTs impart hydrophilicity to the membrane surface, enhance the porosity leading to higher pure water flux and better antifouling behaviour though here too the pore size is not measured [24]. Polyaniline (PANI) nanoparticles were embedded in the PES casting solution and it was observed that the pore size decreased to ~8.0 nm with an increase in the porosity from 62% for the unmodified membrane to 80% for the modified membrane and this was explained due to the small sized PANI nanoparticles [25]. In our previous work, functionalized multiwalled carbon nanotubes were incorporated in PS matrix and the pore dimensions were measured by mercury porometer and it was found that there is a reduction in the size of the pores from ~1.0 μm to 25 nm. This also led to higher water flux and better separation of heavy metals such as Pb(II), Cu(II), Cd(II), As(III) [26]. Separation studies of Cr(IV), As(III), Pb(II) were also been carried out with single-walled carbon nanotubes incorporated PS membranes [27]. Similar reduction in pore dimensions was observed when functionalized single-walled carbon nanotubes were incorporated in the PS matrix. Apart from the separation of heavy metal ions, these membranes also showed selectivity towards removal of heavy metals from binary mixtures of metal ions [28].

The separation characteristics of mixed-matrix membranes are a function of the pore structure, pore dimension and porosity of membranes. However, there is ambiguity regarding the ability of the membrane to separate based on the 'sieving mechanism' or by 'adsorption'. One way of offering a better explanation to this is by understanding the porous nature of the membrane. One of the techniques by which the porous structure of any material can be understood is small angle neutron scattering (SANS) and there are very few SANS studies of the membranes. SANS technique has been used to study the porosity of ultrathin cellulose acetate membranes, that is, active layer membrane [29] and scattering experiment were also performed on cellulose acetate ultrafiltration and reverse osmosis membranes in both the dry state and after swelling the membranes in deuterated solvents, annealed membranes and unannealed membranes.

The importance of CNT/polymer mixed-matrix membranes in desalination and water purification has been excellently reviewed and it has been highlighted that better understanding of the pore size and pore distribution is essential for the membrane performance [30]. The enhanced transport of water through the mixed-matrix membranes containing nanotubes could be due to the channel formation by the linked CNTs even though the pore dimensions are smaller than the pristine membranes as is depicted in the cartoon (Fig. 1).

As can be seen from the limited literature on the porous nature of membranes, the study of pore dimensions, distribution of pores and other morphological studies for functionalized MWCNT/PES membranes and their correlation to the many properties observed assumes importance. In the present study, the MWCNTs were functionalized and incorporated into the PES matrix and membranes cast by the phase inversion process to understand the uniformity of the surface, the formation of uniform pores and pore dimensions and compare the morphological variations observed when they are subjected to analysis by capillary porometry and morphological signatures obtained from neutron light scattering. In-depth analysis of pores were also carried out by soaking the membranes in deuterated water (D_2O) before subjecting the membranes to neutron scattering to get a better contrast. Finally, the impedance studies of pristine membrane and MWCNT incorporated membranes were also compared.

2. Experimental

2.1. Materials

PES Veradel 3300 was a gift sample from M/s Solvay Speciality Polymers Ltd., Vadodara, India. MWCNTs (diameter 6–9 nm) were commercial sample from M/s Sigma-Aldrich (India), the surfactant Brij 98 (Sigma-Aldrich), ethylene diamine (>99%, Sigma-Aldrich) and sodium azide (>99%, Sigma-Aldrich) were used as received.

2.2. Purification and functionalization of MWCNT

2.2.1. Surface cleaning

It is important to purify the commercially purchased nanotubes as it may be associated with some sort of unwanted side product during the preparation of nanotubes. We have used a modified method for the removal of these impurities such as carbon soot, metal ions. First of all 2 g of

nanotubes with 500 mL of 1% Brij 98 (a non-ionic surfactant) were sonicated in the solution for about 2 h. Then this solution was allowed to stand for 6 h and the supernatant liquid was decanted and centrifuged at 3,000 rpm for 15 min. The precipitate was rejected as it contains the soot and nanotubes free from impurities were collected. In order to get the uncontaminated nanotubes, the process was repeated for three times. Washing alternatively with water and brine solution helps to remove the surfactant associated with the nanotubes. In order to remove the heavy metals that may be present still it was treated with 0.5 N HCl solution to by converting it into soluble metal chlorides. The treated nanotubes do not get attracted to magnetic needle which shows the removal of traces of Ni/Co/Fe which were present in the raw nanotubes. Finally cleaned nanotubes were dried in the vacuum oven at 80°C for 10 h. Yield obtained was ~40%.

2.3. Oxidation, amide and azide functionalization of MWCNT

The details of the different functionalized MWCNT are given in Table 1. The functionalizations of purified MWCNT were carried out with three functionality to enhance the interaction between MWCNT and polymer. As carboxylated groups are easy to convert to other functional groups, for example, ester, amide, etc., oxidation step is chosen to start the functionalization [31]. In the first step, fresh nanotubes were treated with 3:1 mixture of concentrated nitric acid and sulphuric acid (40 mL) for 24 h at 33°C. In order to obtain clean surface of oxidized nanotubes, treated nanotubes were washed with deionized (DI) water for five times. Then dry the product in vacuum oven at 80°C for 8 h. Yield obtained was 58.2%. In the next step, acyl group is introduced on nanotubes. 200 mg of oxidized nanotubes are taken and treated with 20 mL of thionyl chloride and 2 mL of N,N-dimethyl formamide (DMF). The reaction was kept under reflux for 36 h at 60°C. The excess thionyl chloride was removed by washing the effluent by toluene. Nanotubes were collected by centrifugation. The sample was then dried in vacuum oven at 80°C for 8 h. Further for amide functionalization, 20 mg of acylated MWCNT was dispersed in 10 mL ethylene diamine and sonication is done for 16 h at 33°C. The reaction mixture was diluted with 200 mL of methanol. Product was dried in vacuum oven at 80°C for 8 h with 70.3% yield. To add azide functional group, 60 mg of acylated MWCNT and 5 mg of sodium azide was added to DMF and reaction was performed at room temperature for 24 h. DMF was used as solvent. The product was dried in vacuum oven at 80°C for 8 h. Yield was 77.5%. Functionalization was confirmed by FTIR analysis.

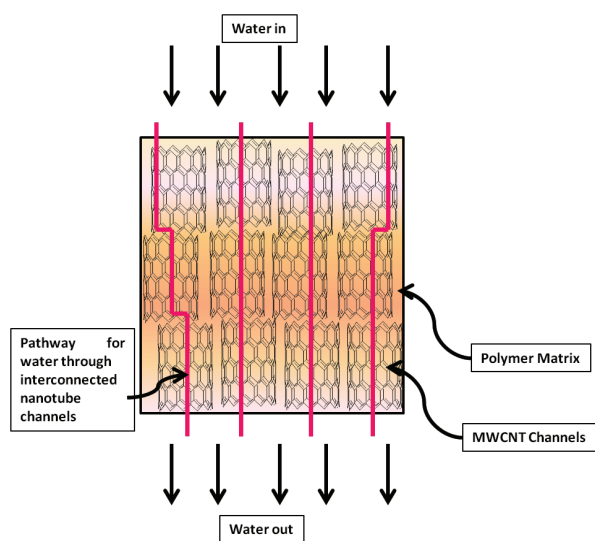


Fig. 1. Pathway of water through mixed-matrix membranes containing MWCNT.

Table 1
Coding of differently functionalized nanotubes

Functional group	Code
Unfunctionalized	C0
Oxidized	C1
Acylated	C2
Azide	C3
Amide	C4

2.4. Incorporation of MWCNT into PES to form mixed-matrix membranes

Primarily, PES was dried in vacuum oven at 80°C for 24 h. DMF was used as solvent to dissolve the polymer. 1% isopropanol in DI water was used as coagulation bath. A solution of 18% PES and 82% DMF was made by dissolving the polymer in the solvent. A viscous solution was formed. Different weight percentage (1% and 2%) of all the functionalized MWCNT was added to the polymer solution. Mixed-matrix membranes were prepared according to the dry/wet phase inversion process. The membrane dope solutions sonicated in an ultrasonic device for 12 h for well dispersion of nanotubes and homogeneity of the solution. Casting of membranes was carried out on a glass plate with the help of casting knife to get film of homogeneous thickness, exposed to air for 10 min for the evaporation of the solvent and immersed in coagulation water bath containing 1% isopropanol where the solvent non-solvent exchange takes place. These membranes were washed with deionized water then dried at 60°C in vacuum oven and kept soaked in deionized water for several days.

3. Characterization

Functionalized MWCNT as well as the functionalized nanotubes incorporated polymeric membranes were analyzed by different analytical techniques. The codes for the different mixed-matrix membrane are given in Table 2. Functionalized MWCNT was analyzed by FTIR spectroscopy to ensure the functionalization of nanotubes with different functionality. The functionalized nanotubes as well as membranes were characterized by thermogravimetric analysis to verify the thermal stability. The structural morphology of the membranes was checked by field emission scanning electron microscopy (FESEM). The porosity of membranes was analyzed by two different techniques. (i) SANS and (ii) capillary flow porometry (Fig. 2).

Pore distribution analyzed by both the techniques was compared.

3.1. Small angle neutron scattering

The SANS experiments were performed on SANS Diffractometer at Dhruva Reactor, Mumbai, India [32]. The instrument utilizes a neutron velocity selector to get a monochromated neutron beam with a mean wavelength of 5.2 Å, with a wavelength resolution ($\Delta\lambda/\lambda$) of approximately 15%. The angular divergence of the incident beam was $\pm 0.5^\circ$.

Table 2
Sample details of the different MWCNT incorporated polyether sulfone membranes

Functionalization of nanotube	MWCNT concentration (%)	Code for membranes
–	–	M1
Oxidized	1.0	M21
Amide	1.0	M31
Amide	2.0	M32
Azide	1.0	M41

The scattered neutrons were detected using a linear He³ position sensitive gas detector. The data were collected over the wave vector range ($Q = 4\pi\sin\theta/\lambda$) of 0.015 – 0.35 Å⁻¹, where 2θ is the scattering angle and λ is the wavelength of incident neutrons. The diffractometer is well suited for the study of a wide variety of system having characteristic dimensions between 10 and 300 Å. The membrane samples were cut into small pieces of 1 × 1.5 cm² dimension and few pieces were put together in the aluminium foil and positioned in the path of the beam. The data analysis was done after the data were corrected for the direct beam and the background contribution.

3.2. Capillary flow porometer

The morphology of the membrane was also confirmed by capillary flow porometer (Porous Materials Inc., USA Model 1100 AEX) at Smita Labs, IIT Delhi. It is an expulsion method where we have considered pores of the membrane as capillary. Wetting fluid used for soaking the membrane is Galwick. The surface tension (γ) of the fluid is 1.59 N/m² which makes zero contact angles with the membrane surface. So the membrane sample wets perfectly so that all the pores were filled with the wetting fluid. Then the gas was passed through the samples and pressure applied and increases gradually till all the fluid was removed from the pores. And gas was allowed to pass through the pores. Larger pores are emptied first followed by the smaller pores. The pressure at which the largest pore emptied and the gas pass through them is called bubble point pressure. Keeping on increasing the pressure, smaller pores were also emptied and gas passes through the pores. Washburn equation which converts the applied pressure into pore diameter was used to calculate the pore characteristic of the sample.

$$D = 4\gamma \cos \theta / P \quad (1)$$

where P is the differential pressure, γ is surface tension, θ is the contact angle and D is the diameter of the pore. In this case, contact angle is zero so we get modified equation from which we calculate the pore diameter.

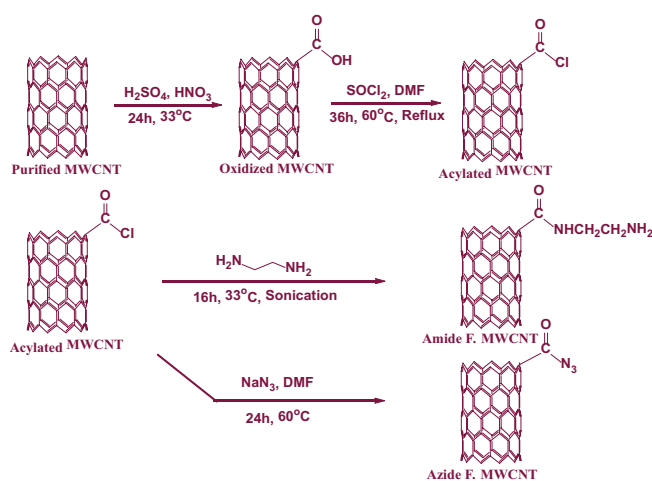


Fig. 2. Schematic representation of different steps of functionalization of MWCNT.

$$D = 4\gamma/P \quad (2)$$

3.3. Impedance measurements

The conducting property of the polymeric mixed-matrix membranes has been measured on Precision LCR Meter E4980A, Agilent (India), within the frequency range 20 Hz to 2 MHz at the Department of Physics, Faculty of Science, the M. S. University of Baroda. The membrane was placed between the two silver electrodes having 0.885 cm² area. The experiment was performed on varying voltages. The AC conductivity (σ) of the membrane was calculated from the impedance data in Siemens per cm unit from the following equation:

$$\sigma = \frac{1}{r_b} \times \frac{t}{A} \quad (3)$$

where r_b is the impedance value obtained from the data. A is the area of the silver electrodes between which membrane should fixed and t is the thickness of the membrane.

3.4. Field emission scanning electron microscopy

Morphological studies were made by FESEM (JSM-7100F, JEOL, India). FESEM analysis was performed at Central Salt and Marine Research Institute, Bhavnagar, Gujarat.

3.5. Scanning electron microscopy

Cross sectional image of membranes was taken by scanning electron microscopy (SEM) at Department of Metallurgical and Materials Engineering, Faculty of Technology & Engineering, the M S University of Baroda.

3.6. Thermogravimetric analysis

The thermal stability of functionalized CNT and membranes was confirmed from thermogravimetric analysis (TGA). TGA data were obtained in hydrogen atmosphere on Star SW 7.01 thermo gravimetric analyser (Mettler Toledo, India) at scan rate of 10°C/min.

4. Results and discussion

4.1. Characterization of functionalized nanotubes

Functionalization of nanotubes was confirmed from FTIR spectroscopy. In Fig. 3, the spectra of oxidized MWCNT as well as purified MWCNT are shown. The peaks obtained in the spectra of oxidized nanotubes at 1,734 cm⁻¹ due to presence of C=O stretching and broad peak at 3,235 cm⁻¹ confirms the presence of –OH functional group at nanotubes hence carboxylic moiety has been successfully added to the MWCNTs. Whereas no such significant peaks are observed in case of purified nanotubes. Thus the nanotubes were found to be functionalized with desired functional group and so were used for further dispersion of these nanotubes in the PES dope solution to prepare the membranes by phase inversion process.

The surface of the nanotubes was sufficiently cleaned by purification process described earlier which can be seen

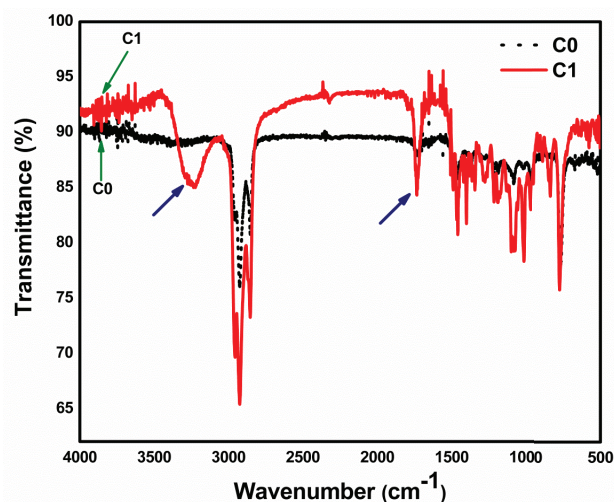


Fig. 3. Infrared spectra of unfunctionalized (C0) and functionalized (C1) nanotubes.

by SEM image (Fig. 4(a)). Oxidized, amide, azide functional groups added to nanotubes have enhanced their interaction with polymer matrix and resulted in better performance of the mixed-matrix membrane, but at the same time it ruptured the surface of MWCNTs at some places (Figs. 4(b)–(d)). However the rupture is limited to the outer most walls of the nanotubes and so the internal walls remained undamaged. This is one of the advantages of using multiwalled nanotubes as tube characteristic are retained even after functionalization which is the limitation of single-walled nanotubes. It is for this reason researchers are more interested in using multiwalled nanotubes as compared with single-walled nanotubes. The micrographs obtained from the FESEM analysis of functionalized MWCNT show that the morphology of the membranes not much differs for dissimilar functionalities (Fig. 4).

4.2. Characterization of membranes

The TGA of the pristine as well as MWCNT incorporated membranes was taken to observe the thermal stability of the membranes (Fig. 5). It was found that thermal stability of mixed-matrix membranes was not adversely affected due to the presence of the functionalized nanotubes and in fact there was a marginal increase in the stability. For example at 550°C, the M1 is degraded by 21% whereas the other membranes M21, M31, M41 all degrade only 17% at the same temperature.

This enhancement is due to the presence of nanotubes in the polymer matrix. Values of initial decomposition temperature are shown in Table 3.

The SEM micrograph of cross section of cold fractured membrane shows the asymmetric nature of membrane (Fig. 6), that is, upper surface contains smaller pores and lower surface contains larger pores.

FESEM images of the surface of the membranes were also taken (Fig. 7), which clearly shows the change in the surface, pore dimensions as well as the porosity of the samples.

As can be seen, the sample becomes much smoother with addition of the nanotubes in the polymer matrix.

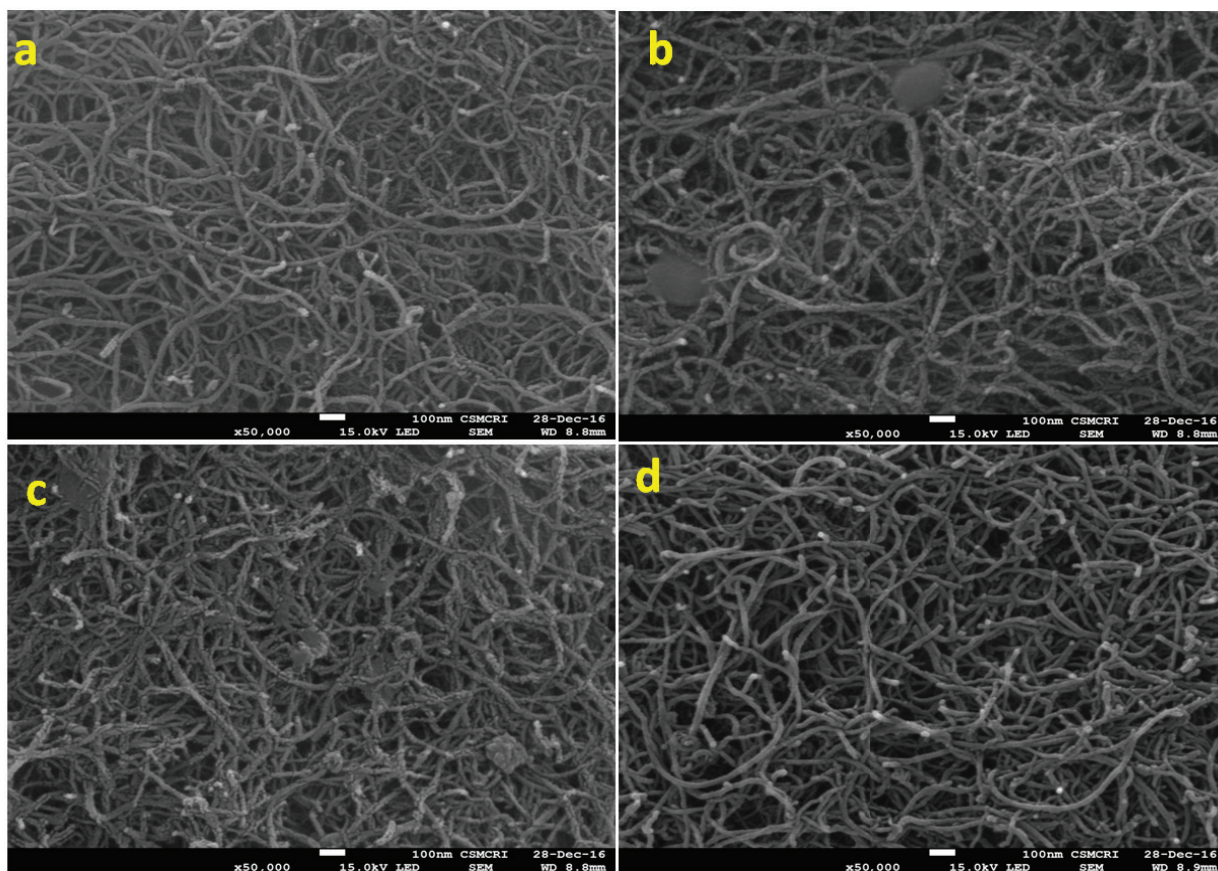


Fig. 4. FESEM micrographs of functionalized MWCNT: (a) oxidized [C1], (b) acylated [C2], (c) azide functionalized [C3] and (d) amide functionalized [C4].

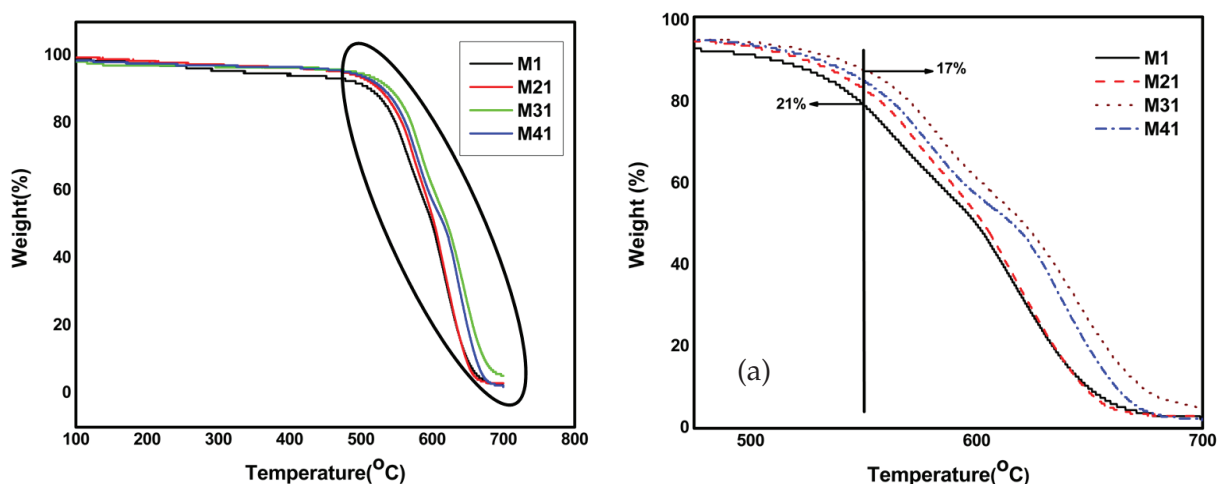


Fig. 5. Thermal stability of mixed-matrix membranes as measured by TGA. (a) Enlarged image.

This result is further supported by the capillary flow porometry as summarized in Table 4.

Capillary flow analysis reveals the pore dimensions of the membranes. The study shows the dimensions of the pore of polymer vary with the addition of MWCNT in the membranes. The largest pore of the membranes was detected by bubble point as by applying the pressure, the pores are

emptied of the Galwick liquid. On applying higher pressure, this liquid was expelled from the other smaller pores also. The bubble point pressure obtained was 33.5 psi and bubble point diameter obtained was 0.19 μ . This data is summarized in Table 4. Comparing the mean flow pore pressure and bubble point pressure for the pristine as well as for the mixed-matrix membranes, we can see that the pressure for

mixed-matrix membrane decreased significantly. Thus, we can conclude that the pores are much more uniform in MWCNT impregnated mixed-matrix membranes than in pristine membranes.

To overcome this limitation of detection of small pores by capillary porometer, a much more detailed structural information of the inorganic filler incorporated polymeric

membranes was studied by the neutron scattering technique namely the SANS. This technique makes use of wave properties of neutron to probe the structure of the material.

In the SANS study, the differential scattering cross section per unit volume (dS/dW) for mono-disperse particles is represented by the expression [33] as follows:

Table 3
Thermal stability of membranes depending on the nature of functionality of the CNTs

Membrane code	Initial decomposition temperature (°C)	T_{10} (°C)
M1	482	496
M21	511	531
M31	518	542
M41	521	552

Table 4
Variation of pore diameter and required pressure of membranes having 1% concentration of MWCNT, M1 (pristine), M21 (oxidized), M31 (amide functionalized), M41 (azide functionalized)

Parameter	M1	M21	M31	M41
Mean flow pore pressure (psi)	47.61	37.55	36.35	39.28
Mean flow pore diameter (μ)	0.14	0.17	0.18	0.16
Bubble point pressure (psi)	33.50	33.21	35.82	33.50
Bubble point diameter (μ)	0.19	0.19	0.18	0.19

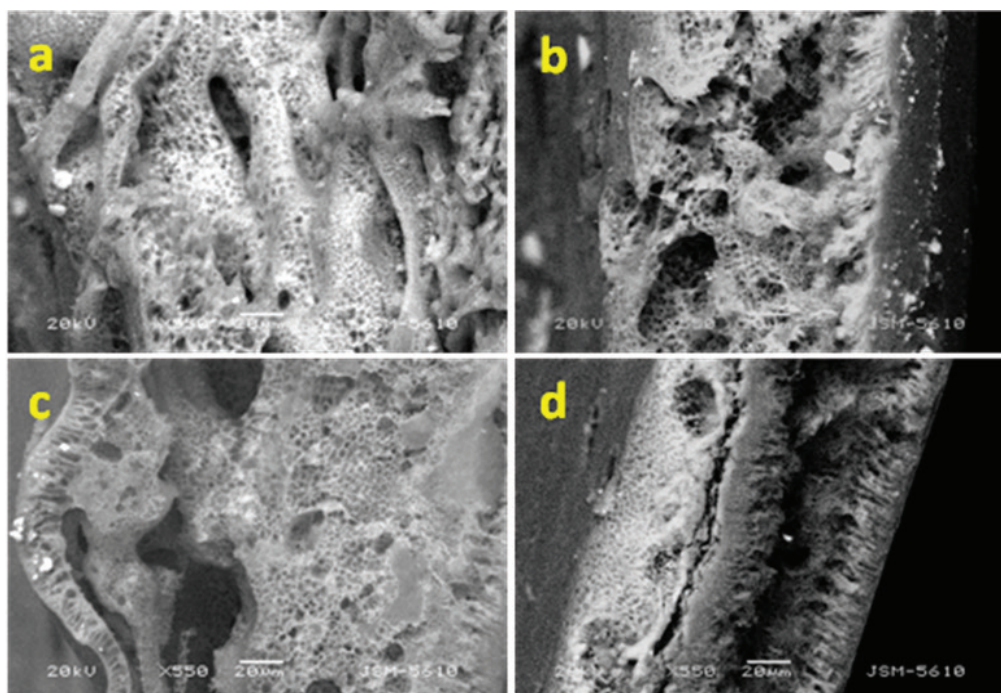


Fig. 6. SEM micrograph of cross section of cold fractured membranes (a) M1, (b) M21, (c) M32 and (d) M41.

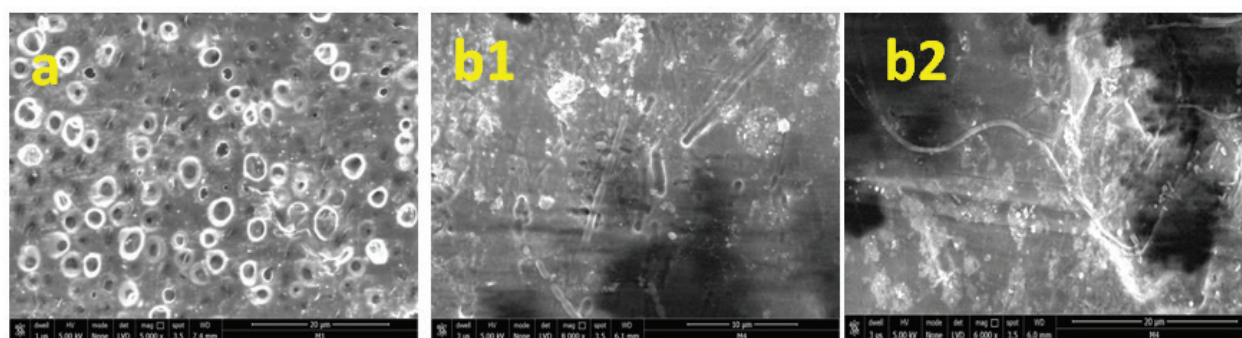


Fig. 7. FESEM images of the surface of the membranes: (a) M1, (b1) M41 (higher magnification) and (b2) M41.

$$\frac{d\Sigma}{d\Omega} = nP(Q)S(Q) + B \quad (4)$$

where n is the number density of the particles, $P(Q)$ is the intraparticle structure factor, $S(Q)$ is the inter-particle structure factor and B is a constant term. $P(Q)$ depends on the shape and size of the particles and $S(Q)$ is decided by the spatial distribution of the particles. For dilute system, $S(Q)$ is considered to be unity. B accounts for the incoherent scattering background that occurs mainly due to the presence of hydrogen in the sample.

For spherical particles/pores of radius R , $P(Q)$ can be given by:

$$P(Q) = \frac{16\pi^2}{9} (\rho_p - \rho_s)^2 R^6 \left[3 \frac{\sin(QR) - (QR)\cos(QR)}{(QR)^3} \right]^2 \quad (5)$$

where ρ_p and ρ_s are the scattering length densities of particle/pore and solvent/matrix, respectively.

The $P(Q)$ of randomly oriented cylindrical particles with the radius R and length L ($=2l$) is given by:

$$P(Q) = \pi^2 R^4 L^2 (\rho_p - \rho_s)^2 \int_0^{\pi/2} \frac{4j_1^2(QR \sin \theta)}{Q^2 R^2 \sin^2 \theta} \frac{\sin^2(Ql \cos \theta)}{Q^2 l^2 \cos^2 \theta} \sin \theta d\theta \quad (6)$$

where $j_1(x)$ is first order Bessel function and q is the angle subtended by the principal axis of the cylinder with Q .

For polydispersed systems, $d\Sigma/d\Omega$ in Eq. (4) can be expressed as follows:

$$\frac{d\Sigma}{d\Omega}(Q) = \int \frac{d\Sigma}{d\Omega}(Q, R) f(R) dR + B \quad (7)$$

where $f(R)$ is the size distribution and usually accounted by log normal distribution as given by:

$$f(R) = \frac{1}{R\sigma\sqrt{2\pi}} \exp \left[-\frac{\left(\ln R/R_{med} \right)^2}{2\sigma^2} \right] \quad (8)$$

where R_{med} and σ are the median value and standard deviation, respectively. The mean (R_m) and median values are related as $R_m = R_{med} \exp(\sigma^2/2)$.

For non-particular structures, randomly distributed two-phase system, the scattering intensity can also be modeled using Ornstein–Zernike model where [34]

$$I(Q) = I_0 \frac{1}{1 + (Q\xi)^2} \quad (9)$$

where I_0 is the forward scattering and ξ is the correlation length. The above-mentioned equation characterizes the

exponential decay of the composition fluctuations correlation function, with correlation length ξ .

The data are analyzed using SASFIT software. Throughout the data analysis, corrections were made for instrumental smearing. The calculated scattering profiles were smeared by the appropriate resolution function to compare with the measured data. Fig. 8 shows the scattering profile of the pure as well as functionalized membranes soaked in the D_2O .

The scattering intensities for the different membrane samples are presented in the arbitrary unit and shifted vertically for the clarity of the presentation. There are two models that are considered: (i) the polydispersed sphere model where the pores are considered to be spherical and surrounded by a matrix material and (ii) the random two-phase model, where first phase is the pores and the second phase the surrounding matrix material. These data are presented in Table 5.

Our data were better fit to the second model where the scattering from the distributed polydispersed spherical pores is combined with OZ equation to fit the experimental data. The correlation length is found to be about 3.9 nm. The addition of the MWCNT influences the SANS data in the intermediate Q range. All these data have been analyzed by considering the scattering contributions from the CNTs along with that from the distributed pores. The MWCNT radius is found to be about 4 nm while the length of the CNTs (in microns) cannot be estimated due to the limited Q range of the data. A fixed value of the MWCNT length (~100 nm) more than the

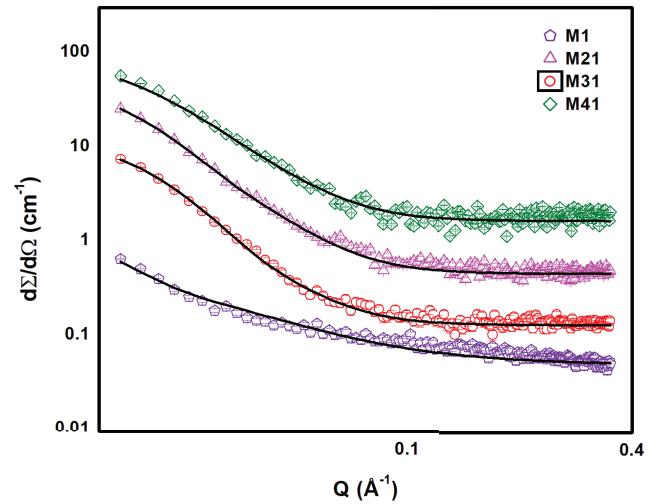


Fig. 8. SANS profile of membrane soaked in D_2O .

Table 5

SANS data of membrane soaked in D_2O containing 1% concentration of MWCNT, M1 (pristine), M21 (oxidized), M31 (amide functionalized), M41 (azide functionalized)

Sample	Pore radius (nm)	Polydispersity (σ)	Correlation length (nm)
M1	14.8	0.27	3.9
M21	9.7	0.27	3.9
M31	8.3	0.29	3.9
M41	7.4	0.27	3.9

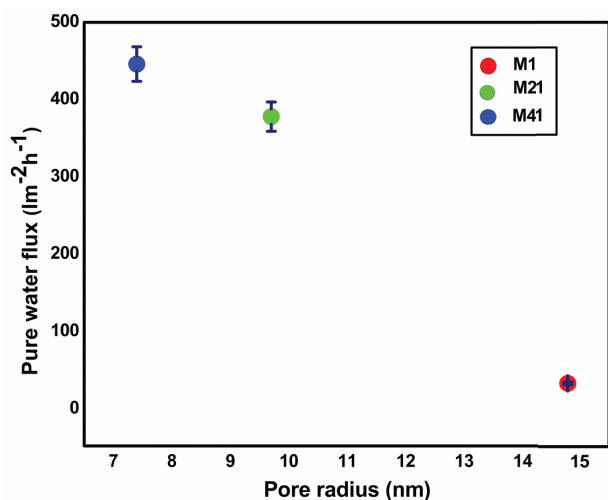


Fig. 9. Plot of pure water flux vs. pore radius of membranes.

$2\pi/Q_{\min}$ has been used through the data analysis. The fitted parameters are listed in Table 5. It may be pointed out that the distribution of the pores does not change with addition of the MWCNT while the pore radius reduces significantly.

From the membrane performance data of our previous work, we have found that pure water flux of the membranes increases as the pore size of the membranes decreases. The maximum value of pure water flux is $446 \text{ L m}^{-2} \text{ h}^{-1}$ of mixed-matrix membrane containing azide functionalized multiwalled carbon nanotubes having pore diameter of 7.4 nm. The plot of pure water flux vs. pore diameter is shown in Fig. 9.

A small piece of membrane was characterized by the electrochemical impedance analyzer. Pristine PES membrane and functionalized MWCNT mixed-matrix membrane were analyzed by the LCR meter. In the case of pristine membrane, we have observed nearly constant phase angle so we are not getting ac conductivity. This observation may be attributed to the solid packed structure of PES and no filler or charge carrier in the polymer structure which can result into transport or conduction process. Therefore no ac conductivity is observed. However, it may provide high dc conductivity or insulating character. While in the case of mixed-matrix membranes which contains functionalized MWCNT as filler material, Z' (real impedance) was plotted against Z'' (imaginary impedance) which gives a semicircle curve (Fig. 10). Such semicircle attributes the parallel combination of bulk resistance and capacitance of the mixed-matrix film. When this film was subjected to variation of temperatures, no change in bulk resistance was observed. But with the change of biasing voltage across the film starting from 400 to 900 mV, the bulk impedance of the film decreases maintaining the semicircle character. On increasing the voltage there is decrease in the impedance value hence increases the conductivity. The conductivity values are summarized in Table 6.

Conductivity is changing because of the release of the trapped electrons between the MWCNT. When the voltage is increased, more trapped electrons are released to provide the lower resistance/impedance. This confirms the presence of functionalized MWCNT in the polymer matrix of the membrane and this also shows the successful functionalization of

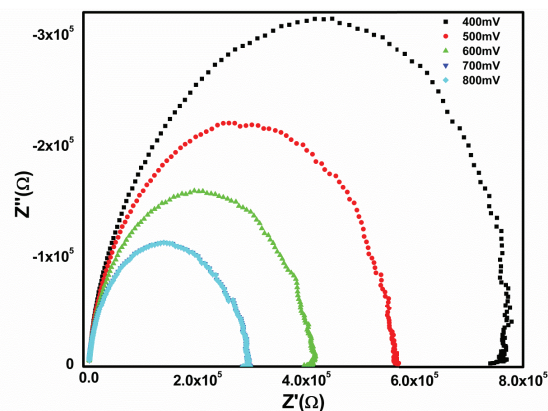


Fig. 10. Impedance spectra of mixed-matrix membrane (M32).

Table 6
Conductivity of mixed-matrix membrane (M32) at different voltages

S. No.	Voltage (mV)	Conductivity (S/cm)
1	400	1.84×10^{-8}
2	500	2.17×10^{-8}
3	600	2.96×10^{-8}
4	700	3.59×10^{-8}
5	800	5.70×10^{-8}

the MWCNT. Thus we may conclude that the mixed-matrix membrane is thermally insulating while electrically conducting.

5. Conclusions

Our studies show that the incorporation of nanotubes has resulted in enhancement of all relevant factors such as porosity, flux and thermal stability. These studies also highlight that the nanotubes form linked channels which explains the higher flux for those reported in our previous studies as well as in other investigations. The SANS study reported here indicates that there could be alignment of the nanotubes parallel to the membrane surface resulting from the phase inversion process. This observation is also supported by the impedance studies that show enhanced conductivity. Further conclusive establishment of the alignment of nanotubes needs investigations which are in progress.

Acknowledgement

This work was supported by UGC-DAE (grant CRS-M-193).

Symbols

D	—	Diameter of the pore
P	—	Differential pressure
γ	—	Surface tension
θ	—	Contact angle
σ	—	Conductivity of the membranes
r_b	—	Impedance

t	—	Thickness of the membranes
A	—	Area of the silver electrodes
dS/dW	—	Differential cross section per unit volume
n	—	Number density of the particles
$P(Q)$	—	Intra-particle structure factor
$S(Q)$	—	Inter-particle structure factor
B	—	Constant term
R	—	Pore radius
ρ_p	—	Scattering length densities of particle/pore
ρ_s	—	Scattering length densities of solvent/matrix
$j_1(x)$	—	First order Bessel function
θ	—	Angle subtended by the principal axis of the cylinder with Q
$f(R)$	—	Size distribution
R_{med}	—	Median value
σ	—	Standard deviation
R_m	—	Mean value
I_0	—	Forward scattering
ξ	—	Correlation length

References

- [1] C. Zhao, J. Xue, F. Ran, S. Sun, Modification of polyethersulfone membranes – a review of methods, *Prog. Mater. Sci.*, 58 (2013) 76–150.
- [2] V. Bruggen, Chemical modification of polyethersulfone nanofiltration membranes: a review, *J. Appl. Polym. Sci.*, 114 (2009) 42–630.
- [3] D. Zhao, S. Yu, A review of recent advance in fouling mitigation of NF/RO membranes in water treatment: pretreatment, membrane modification, and chemical cleaning, *Desal. Wat. Treat.*, 55 (2015) 870–891.
- [4] S. Loeb, S. Sourirajan, Sea water Demineralization by Means of an Osmotic Membrane, in *Advances in Chemistry*, American Chemical Society, Washington, D.C., 1963.
- [5] J.E. Cadotte, M.J. Steuck, R.J. Petersen, NTIS Report No. PB-288387, loc. cit, 1978.
- [6] C. Zimmerman, A. Singh, W. Koros, Tailoring mixed matrix composite membranes for gas separations, *J. Membr. Sci.*, 137 (1997) 145–154.
- [7] N. Srivastava, K.V. Joshi, A.K. Thakur, S.K. Menon, V.K. Shahi, BaCO₃ nanoparticles embedded retentive and cation selective membrane for separation/recovery of Mg²⁺ from natural water sources, *Desalination*, 352 (2014) 142–149.
- [8] A.L. Ahmad, A.A. Abdulkarim, S. Ismail, O. B. Seng, Optimization of PES/ZnO mixed matrix membrane preparation using response surface methodology for humic acid removal, *Korean J. Chem. Eng.*, 33 (2016) 997–1007.
- [9] L. Yu, Y. Zhang, Y. Wang, H. Zhang, J. Liu, High flux positively charged loose nanofiltration membrane by blending with poly (ionic liquid) brushes grafted silica spheres, *J. Hazard. Mater.*, 287 (2015) 373–383.
- [10] Q. Zhao, J. Hou, J. Shen, J. Liu, Y. Zhang, Long-lasting antibacterial behavior of a novel mixed matrix water purification membrane, *J. Mater. Chem. A*, 3 (2015) 18696–18705.
- [11] S. Zinadini, A.A. Zinatizadeh, M. Rahimi, V. Vatanpour, H. Zangeneh, Preparation of a novel antifouling mixed matrix PES membrane by embedding graphene oxide nanoplates, *J. Membr. Sci.*, 453 (2014) 292–301.
- [12] T.L.S. Silva, S. Morales-Torres, J.L. Figueiredo, A.M.T. Silva, Multi-walled carbon nanotube/PVDF blended membranes with sponge- and finger-like pores for direct contact membrane distillation, *Desalination*, 357 (2015) 233–245.
- [13] S. Zhao, Z. Wang, J. Wang, S. Yang, S. Wang, PSf/PANI nanocomposite membrane prepared by in situ blending of PSf and PANI/NMP, *J. Membr. Sci.*, 376 (2011) 83–95.
- [14] J. Zhu, N. Guo, Y. Zhang, L. Yu, J. Liu, Preparation and characterization of negatively charged PES nanofiltration membrane by blending with halloysite nano tubes grafted with poly(sodium 4-styrenesulfonate) via surface-initiated ATRP, *J. Membr. Sci.*, 465 (2014) 91–99.
- [15] J.K. Holt, H.G. Park, Y. Wang, M. Stadermann, A.B. Artyukhin, C.P. Grigoropoulos, A. Noy, O. Bakajin, Fast mass transport through sub-2 nanometer carbon nanotubes, *Science*, 312 (2006) 1034–1037.
- [16] Y. Li, G. He, S. Wang, S. Yu, F. Pan, H. Wu, Z. Jiang, Recent advances in the fabrication of advanced composite membranes, *J. Mater. Chem. A*, 1 (2013) 10058–10077.
- [17] B. Corry, Designing carbon nanotube membranes for efficient water desalination, *J. Phys. Chem. B*, 112 (2008) 1427–1434.
- [18] F. Du, L. Qu, Z. Xia, L. Feng, L. Dai, Membranes of vertically aligned superlong carbon nanotubes, *Langmuir*, 27 (2011) 8437–8443.
- [19] T. Altalhi, M.G. Markovic, N. Han, S. Clarke, D. Losic, Synthesis of carbon nanotube (CNT) composite membranes, *Membranes*, 1 (2011) 37–47.
- [20] S. Raganath, S. Mitra, Carbon nanotube immobilized composite hollow fiber membranes for extraction of volatile organics from air, *J. Phys. Chem. C*, 119 (2015) 13231–13237.
- [21] S. Gahlot, V. Kulshrestha, Dramatic improvement in water retention and proton conductivity in electrically aligned functionalized CNT/SPEEK nanohybrid PEM, *ACS Appl. Mater. Interfaces*, 7 (2015) 264–272.
- [22] H.J. Kim, K. Choi, Y. Baek, D.G. Kim, J. Shim, J. Yoon, J.C. Lee, High-performance reverse osmosis CNT/Polyamide nanocomposite membrane by controlled interfacial interactions, *ACS Appl. Mater. Interfaces*, 6 (2014) 2819–2829.
- [23] E. Celik, H. Park, H. Choi, H. Choi, Carbon nanotube blended polyethersulfone membranes for fouling control in water treatment, *Water Res.*, 45 (2011) 274–282.
- [24] E. Celik, L. Liu, H. Choi, Protein fouling behavior of carbon nanotube/polyethersulfone composite membranes during water filtration, *Water Res.*, 45 (2011) 5287–5294.
- [25] S. Zhao, Z. Wang, J. Wang, S. Wang, Poly(ether sulfone)/Polyaniline nanocomposite membranes: effect of nanofiber size on membrane morphology and properties, *Ind. Eng. Chem. Res.*, 53 (2014) 11468–11477.
- [26] P. Shah, C.N. Murthy, Studies on the porosity control of MWCNT/polysulfone composite membrane and its effect on metal removal, *J. Membr. Sci.*, 437 (2013) 90–98.
- [27] S. Gupta, D. Bhatiya, C.N. Murthy, Metal removal studies by composite membrane of polysulfone and functionalized single-walled carbon nanotubes, *Sep. Sci. Technol.*, 50 (2015) 421–429.
- [28] S. Mangukiyi, S. Prajapati, S. Kumar, V.K. Aswal, C.N. Murthy, Polysulfone-based composite membranes with functionalized carbon nanotubes show controlled porosity and electrical conductivity, *J. Appl. Polym. Sci.*, 133 (2016) 43778.
- [29] S. Kulkarni, S. Krause, G.D. Wignall, B. Hammouda, Investigation of the pore structure and morphology of cellulose acetate membranes using small-angle neutron scattering. 1. Cellulose acetate active layer membranes, *Macromolecules*, 27 (1994) 6777–6784.
- [30] S. Kar, R.C. Bindal, P.K. Tewari, Carbon nanotube membranes for desalination and water purification: challenges and opportunities, *Nano Today*, 7 (2012) 385–389.
- [31] M. Majumder, N. Chopra, B.J. Hinds, Effect of tip functionalization on transport through vertically oriented carbon nanotube membranes, *J. Am. Chem. Soc.*, 127 (2005) 9062–9070.
- [32] V.K. Aswal, P.S. Goyal, Small-angle neutron scattering diffractometer at dhruva reactor, *Curr. Sci.*, 79 (2000) 947–953.
- [33] J.S. Pedersen, Analysis of small-angle neutron scattering data from colloids and polymer solutions: modeling and least-square fitting, *Adv. Colloid Interface Sci.*, 70 (1997) 171.
- [34] P. Debye, A.M. Bueche, Scattering by an inhomogeneous solid, *J. Appl. Phys.*, 20 (1949) 518–525.